SUPPLEMENTAL METHODS

Animals: In all perfused tubule experiments, mice were euthanized by cervical dislocation. In all other experiments, mice were anesthetized with 1-2% isofluorane/100% O_2. The Institutional Animal Care and Use Committee at Emory University approved all treatment protocols.

Measurement of serum aldosterone, arterial blood gases and serum electrolytes: Arterial blood was collected through the abdominal aorta under anesthesia with 1-2% isofluorane in 100% O_2. Serum aldosterone concentration was measured by radioimmunoassay at the Cardiovascular Pharmacology Research Laboratory, University of Iowa College of Pharmacy. Serum electrolytes and arterial blood gases were measured using an iSTAT System (Abbot Point of Care, Princeton, NJ).

In vitro perfusion of isolated CCDs: CCDs were dissected from medullary rays and perfused and bathed at flow rates of 2-3 nl/min in the presence of a symmetric, HCO_3^--buffered physiological solution containing in mM: 125 NaCl, 24 $NaHCO_3$, 2.5 K_2HPO4, 2 $CaCl_2$, 1.2 $MgSO_4$ and 5.5 glucose. Tubules were equilibrated at 37°C for 30 min prior to starting the collections. Stock solutions of benzamil hydrochloride (3×10^{-3} M) and bafilomycin (10^{-5} M) were prepared in water and absolute ethanol, respectively. A hydrochlorothiazide stock solution (10^{-1} M) was prepared in DMSO. All chemicals were purchased from Sigma-Aldrich, St. Louis, MO.

Measurement of net transepithelial Cl^- flux. Cl^- concentration was measured in perfusate and collected samples using a continuous-flow fluorimeter and the Cl^- sensitive fluorophore, 6 methoxy-N-(3-sulfopropyl) quinolinium (SPQ; Molecular Probes, Eugene, OR), as described previously (1). Transepithelial Cl^- flux, J_{Cl}, was calculated according to the equation:

$$J_{Cl} = (C_o - C_L)Q/L$$

where C_o and C_L are perfusate and collected fluid Cl^- concentrations, respectively. Q is flow rate in nl/min. L is tubule length. Net fluid transport was taken to be zero since net fluid flux has not been observed in CCDs when perfused in vitro in the presence of symmetric solutions and in the absence of vasopressin (2, 3).

Measurement of transepithelial HCO_3^- flux, J_{tCO2}: Total CO_2 (HCO_3^- + H_2CO_3 + CO_2) concentration, which is mainly HCO_3^- in most physiological solutions, was measured in the perfusate and in collected samples using a continuous-flow fluorimeter with the method of Zhou et al. (4, 5). Transepithelial total CO_2 flux, J_{tCO2}, was calculated as above. Both J_{tCO2} and J_{Cl} were expressed in pmol/mm/min.

Transepithelial voltage (V_T) was measured in the perfusion pipette connected to a high impedance electrometer through an agar bridge saturated with 0.16 M NaCl and a calomel cell as described previously (6). The reference was an agar bridge from the bath to a calomel cell.

***Immunohistochemistry, Imunofluorescence and Quantative Analysis of Immunohistochemistry*:**

For all single and double labeling experiments, we used antibodies to aquaporin 2 (7), *Nedd4-2* (8), pendrin (9), AE1 (Alpha diagnostic International, San Antonio, TX, Catalogue #AE11-A), barttin (10), AE4 (11), and the α4 subunit of the H^+-ATPase (12), all of which have been described previously. The bartin, AE4 and α4-H^+-ATPase antibodies were generous gifts of Drs. Thomas Jentsch, Christian Hubner and Fiona Karet, respectively.

We used Cre reporter mice (dTomato mice, Jackson Labs, #7909) to explore the extent of Cre recombinase expression within the CCD of the intercalated cell *Nedd4-2* null mice. Thus, intercalated

cell *Nedd4-2* null mice were bred with dTomato homozygotes and the resultant offspring studied. To localize Cre recombinase in the intercalated cells, kidneys from these offspring were fixed *in situ* with 4% paraformaldehyde (PFA) in 0.1M phosphate buffer saline (PBS) and post-fixed for 4 hr in 4% PFA at 4°C. Kidneys were cryoprotected in 30% sucrose overnight at 4°C and frozen quickly in optimal cutting temperature (OCT) compound (Tissue-Tek) by immersion in a mixture of dry ice and 2-Methybutane. 5 μm-thick sections were quenched with 50 mM ammonium chloride to reduce autofluorescence and washed in PBS, blocked with Dako serum free ready-to-use protein block (Agilent, Santa Clara, CA) and incubated overnight at 4°C in both anti-pendrin and anti-AE1 antibodies diluted in Dako antibody diluent (Agilent) at 1:3000 and 1:5000, respectively. Sections were then washed and incubated with affinity purified Dylight 488-conjugated goat anti-rabbit IgG antibody (Vector Laboratories, Burlingame, CA) diluted at 1:150 in PBS and incubated for 30 min in dim light at room temperature. Sections were washed, mounted in Prolong Gold antifade (Invitrogen, Carlsbad, CA) and imaged using a Zeiss Axioskop 2 Plus Fluorescence with dual AxioCam HR cameras.

For standard immunohistochemistry, kidneys were fixed *in situ* and embedded in paraffin or polyester wax [polyethylene glycol 400 distearate (Polysciences, Warrington, PA) and 10% 1-hexadecanol] as described previously (13). Immunoreactivity was detected using immunoperoxidase procedures. Blocking was done with 3% H_2O_2 in methanol for 30 minutes, followed by protein blocking using 1% bovine serum albumin, 0.2% gelatin, 0.05% saponin solution. Sections were incubated in the primary antibody diluted in PBS overnight at 4°C. Sections were rinsed with 0.1% BSA, 0.05% saponin and 0.2% gelatin in PBS and incubated with horseradish peroxidase-conjugated goat anti-rabbit secondary antibody (1:200, DAKO) for 2h, washed with PBS and incubated with diaminobenzidine (DAB substrate kit, Vector). Sections were washed in with distilled water, counter stained with hematoxylin, dehydrated with graded ethanols and xylene, mounted and observed by light microscopy.

Double immunolabeling was done using sequential immunoperoxidase procedures as described previously (14). Tissue sections were labeled with the anti-*Nedd4-2* antibody. After the DAB reaction, sections were washed in PBS and blocked again using 3% H_2O_2 in methanol. A second immunolabeling procedure was done on the same sections using the AQP2 as the primary antibody and Vector SG (Vector Laboratories, Burlingame, CA) for the peroxidase substrate, which produces a blue reaction product easily distinguished from the DAB brown reaction product. Sections were then washed with glass distilled water, dehydrated with graded ethanols and xylene, mounted, and observed by light microscopy.

Transporter subcellular distribution was quantified as described previously in bright field light micrographs (15). High-resolution digital micrographs were taken of defined tubule segments using a Leica DM2000 microscope and a Leica DFC425 digital camera (14.4-megapixel images, 63X objective) and Leica DFC Twain Software and LAS application suite (Leica Microsystems, Buffalo Grove, IL). Pixel intensity across a line drawn from the tubule lumen through the center of an individual cell was quantified with NIH ImageJ, version 1.34s software. Background pixel intensity was calculated as the mean pixel intensity outside the cell and was subtracted from the pixel intensity at each point. Total cellular expression was determined by integrating net pixel intensity across the entire cell. Cell height was determined as the distance in pixels between the apical and the basolateral edges of the cell. Immunoreactivity expressed at zones throughout the cell was determined by integrating pixel intensity at this region. The individual performing the microscopy and quantifying the results was blinded as to the treatment group of each animal. Data from all cells in the CCD of a given subtype, i.e. type A and type B intercalated cells, were averaged for each animal and used in the statistical analysis.

***Immunogold cytochemistry with morphometric analysis*:**

Kidneys were prepared for electron microscopy as described previously (16). Pendrin immunoreactivity was localized in ultrathin sections using immunogold cytochemistry (16, 17). Type B and Non-A, non-B intercalated cells in the CCD were identified using morphological characteristics established in studies of the mouse under basal conditions along with the presence of pendrin immunolabel (16). Apical plasma membrane boundary length, cytoplasmic area and gold label touching the apical plasma membrane and gold label in the cytoplasm, including cytoplasmic vesicles were quantified in type B and Non-A, non-B intercalated cells as described previously (16). For each animal, at least 5 cells in each subtype were selected at random and photographed at a primary magnification of X 15,000 and examined at a final magnification of ~ X 36,000. Raw morphometric data from individual cell profiles were pooled to generate an average value for each cell type for each animal. The "n" reported reflects the number of mice studied.

Quantitative PCR

Kidneys were harvested, immediately snap frozen in liquid nitrogen and stored at -80 ^{o}C, and then homogenized in 300uL of TRIzol reagent (Invitrogen, Hopkinton, MA). RNA extraction was performed using the manufacturer's instructions. To remove DNA, samples were then incubated with DNase I (Thermo Scientific, Waltham, MA) and Reaction Buffer with $MgCl_2$ for DNase I (10X) (Thermo Scientific, Waltham, MA) at 37 ^{o}C for 30 min. 1 μl of EDTA was added and the mixture was incubated again at 65 ^{o}C for 10 min.

Reverse transcription was performed using the Thermoscript RT-PCR kit (Invitrogen, Carlsbad, CA). Quantitative PCR was performed using a Bio-Rad cycler (Hercules, CA) with SYBR Green PCR Reagents (Bio-Rad, Hercules, CA). The following cycle parameters were used: 95°C for 1 min and 40 cycles at 95°C for 20 s, 55°C for 30 s, and 72°C for 30 s. The quantification cycle (Cq) values was defined

as the number of cycles required for the fluorescence signal to exceed the detection threshold. Individual mRNA expression was standardized to 18S gene, and expression was calculated as the difference between the threshold values of the two genes (2-ΔΔCq). Melting curve analysis was always performed during qPCR to analyze and verify the specificity of the reaction. With each sample, the assay was performed in triplicate. The results of these triplicate measurements were averaged to get a single value for each mouse that was used in the analysis.

Primers:
mouse Pendrin (NM_011867.3):
F 5' GACTGTAAAGACCCTCTTGATCTGA 3',
R 5' GGAAGCAAGTCTACGCATGG 3';
Amplicon 90

mouse 18S (X00686):
F 5'-CGG CTA CCA CAT CCA AGG AAG G-3',
R 5'-CCC GCT CCC AAG ATC CAA CTA C-3'.
Amplicon 101

Immunoblots:

Immunoblots of kidney lysates were performed using methods reported previously (18, 19). Whole kidney lysates were isolated by harvesting mouse kidneys and placing them in an ice cooled buffer (0.3 M sucrose, 25 mM imidazole, pH 7.2, containing 1x Roche Complete Protease Inhibitor Cocktail). Tissue was immediately homogenized using an Omni THQ Tissue Homogenizer (Omni International) and then centrifuged at 1000 x g for 15 min at 4^{o}C. To prepare whole cell lysates, intercalated cells were homogenized in Gentle Lysis Buffer (10 mM Tris·HCl, 10 mM NaCl, 2 mM EDTA, 0.5% NP-40, 1% glycerol, and Na_3VO_4 and freshly added 0.18 μg/ml Na_3VO_4, 10 μg/ml PMSF, 5 μg/ml aprotinin, and 1 μg/ml leupeptin). To enable equal protein loading in each lane, protein content in the soluble fraction of

homogenates was measured using a RC-PC protein assay kit (DC Protein Assay Kit, Bio-Rad, Hercules, CA) and then dissolved in Laemmli buffer.

Aliquots containing equal amounts of protein from these lysates were separated by SDS-PAGE on 8.5% acrylamide gels and then electroblotted to PVDF membranes (Immobilon, Millipore, Bedford, MA). Blots were blocked with Odyssey Blocking Buffer (LI-COR Biosciences) following the manufacturer's instructions and then incubated with primary antibody overnight at 4°C, followed by incubation for 2 hours at room temperature with Alexa Fluor 680-linked anti-rabbit IgG (Invitrogen). Pendrin protein was detected by immunoblot using a rabbit anti-rat pendrin antibody described previously (9). To correct for possible differences between lanes in lysate protein loading, membranes were Coomassie stained as reported previously (20). Signals were visualized with an Odyssey Infrared Imaging System (LI-COR Biosciences). Immunoblot and Coomassie band densities were quantified using software program Image J (NIH, available at http://rsb.info.nih.gov/). Pendrin band density was normalized to the density of the Coomassie gel band with the same mobility. To quantify NDCBE renal protein abundance, immunoblots of kidney membrane lysates were performed as described previously (21).

Blood pressure measurements:

Blood pressure was measured in conscious mice by telemetry using methods we have reported previously (18, 22). These measurements were made by an observer that was blinded as to the genotype of each mouse. Systolic blood pressure was also measured in conscious mice by tail cuff using a B-2000 (Visitech Systems), as we reported previously (15). To condition mice for tail cuff blood pressure readings, animals were placed in a platform for 15 min on 2 consecutive days. Over the next 3-4 consecutive days, mice were placed on the platform and at least four readings were taken. All conditioning and all blood pressure readings were performed at the same location under quiet, low-light

conditions. Measurements and conditioning were performed by the same operator at the same time of day.

Statistical Analysis:

For each CCD perfused in vitro, one to two replicate J_{tCO2} or J_{Cl} measurements were made under each condition. The flux reported for each mouse represents the mean of all replicate measurements made under that condition. The "n" reported represents the number of mice studied. Just 1 tubule was studied per mouse. In quantitative immunohistochemistry experiments, for each mouse studied label was quantified in 8-16 cells from each cell subtype. For immunogold studies, gold label was quantified in 5-12 type B intercalated cells and in 5-18 non-A, non-B intercalated cells from each mouse. In each mouse studied, these replicates were averaged to get a single value for each cell type. When comparing two groups, statistical significance was determined using a paired or unpaired two-tailed Student's t test, as appropriate. Data are displayed as the mean ± SEM.

REFERENCES

1. Garcia NH, Plato CF, and Garvin JL. Fluorescent determination of chloride in nanoliter samples. *Kidney Int.* 1999;55(321-5.

2. Knepper MA, Good DW, and Burg MB. Ammonia and bicarbonate transport by rat cortical collecting ducts perfused in vitro. *AmJPhysiol.* 1985;249(F870-F7.

3. Knepper MA, Good DW, and Burg MB. Mechanism of ammonia secretion by cortical collecting ducts of rabbits. *AmJPhysiol.* 1984;247(F729-F38.

4. Pech V, Zheng W, Pham TD, Verlander JW, and Wall SM. Angiotensin II activates H+-ATPase in type A intercalated cells in mouse cortical collecting duct. *JAmSocNephrol.* 2008;19(84-91.

5. Zhou Y, Bouyer P, and Boron WF. Role of tyrosine kinase in the CO_2-induced stimulation of HCO_{3-} reabsorption by rabbit S2 proximal tubules. *AmJPhysiol.* 2006;291(F358-F67.

6. Wall SM. NH_4^+ augments net acid secretion by a ouabain-sensitive mechanism in isolated perfused inner medullary collecting ducts. *AmJPhysiol.* 1996;270(F432-F9.

7. DiGiovanni SR, Nielsen S, Christensen EI, and Knepper MA. Regulation of collecting duct water channel expression by vasopressin in Brattleboro rat. *ProcNatlAcadSciUSA.* 1994;91(8984-8.

8. Flores SY, Loffing-Cueni D, Kamynina E, Daidie D, Gerbex C, Chabanel S, Dudler J, Loffing J, and Staub O. Aldosterone-induced serum and glucocorticoid-induced kinase 1 expression is accompanied by Nedd4-2 phosphorylation and increased Na+ transport in cortical collecting duct cells. *JAmSocNephrol.* 2005;16(2279-87.

9. Knauf F, Yang C-L, Thomson RB, Mentone SA, Giebisch G, and Aronson PS. Identification of a chloride-formate exchanger expressed on the brush border membrane of renal proximal tubule cells. *ProcNatlAcadSciUSA.* 2001;98(9425-30.

10. Estevez R, Boettger T, Stein V, Birkenhager R, Otto E, Hildebrandt F, and Jentsch TJ. Barttin is a Cl^- channel β subunit-crucial for renal Cl- reabsorption and inner ear K^+ secretion. *Nature.* 2001;414(558-61.

11. Chambrey R, Kurth I, Peti-Peterdi J, Houillier P, Purkerson JM, Leviel F, Hentschke M, Zdebik AA, Schwartz GJ, Hubner CA, et al. Renal intercalated cells are rather energized by a proton than a sodium pump. *Proc Natl Acad Sci U S A.* 2013;110(19):7928-33.

12. Dou H, Xu J, Wang Z, Smith AN, Soleimani M, Karet FE, Greinwald JH, and Choo D. Co-expression of pendrin, vacuolar H+-ATPase a4-subunit and carbonic anhydrase II in epithelial cells of the murine endolymphatic sac. *JHistochemCytochem.* 2004;52(1377-84.

13. Kim Y-H, Pham TD, Zheng W, Hong S, Baylis C, Pech V, Beierwaltes WH, Farley DB, Braverman LE, Verlander JW, et al. Role of pendrin in iodide balance: going with the flow. *AmJPhysiol.* 2009;297(1069-79.

14. Kim Y-H, Verlander JW, Matthews SW, Kurtz I, Shin WK, Weiner ID, Everett LA, Green ED, Nielsen S, and Wall SM. Intercalated cell H+/OH- transporter expression is reduced in *Slc26a4* null mice. *AmJPhysiol.* 2005;289(F1262-F72.

15. Verlander JW, Hong S, Pech V, Bailey JL, Agazatian D, Matthews SW, Coffman TM, Le T, Inagami T, Whitehill FM, et al. Angiotensin II acts through the angiotensin 1a receptor to upregulate pendrin. *AmJPhysiol.* 2011;301(F1314-F25.

16. Wall SM, Hassell KA, Royaux IE, Green ED, Chang JY, Shipley GL, and Verlander JW. Localization of pendrin in mouse kidney. *AmJPhysiol.* 2003;284(F229-F41.

17. Verlander JW, Hassell KA, Royaux IE, Glapion DM, Wang ME, Everett LA, Green ED, and Wall SM. Deoxycorticosterone upregulates PDS (Slc26a4) in mouse kidney: role of pendrin in mineralocorticoid-induced hypertension. *Hypertension.* 2003;42(3):356-62.

18. Kim Y-H, Pech V, Spencer KB, Beierwaltes WH, Everett LA, Green ED, Shin WK, Verlander JW, Sutliff RL, and Wall SM. Reduced ENaC expression contributes to the lower blood pressure observed in pendrin null mice. *AmJPhysiol.* 2007;293(F1314-F24.

19. Klein JD, Martin CF, Kent KJ, and Sands JM. Protein kinase C-alpha mediates hypertonicity-stimulated increase in urea transporter phosphorylation in the inner medullary collecting duct. *Am J Physiol Renal Physiol.* 2012;302(9):F1098-103.

20. Welinder C, and Ekblad L. Coomassie staining as loading control in western blot analysis. *JProteome Res.* 2011;10(1416-9.

21. Sinning A, Radionov N, Trepiccione F, Lopez-Cayuqueo KI, Jayat M, Baron S, Corniere N, Alexander RT, Hadchouel J, Eladari D, et al. Double Knockout of the Na+-Driven Cl-/HCO3-Exchanger and Na+/Cl- Cotransporter Induces Hypokalemia and Volume Depletion. *J Am Soc Nephrol.* 2017;28(1):130-9.

22. Pech V, Pham TD, Hong S, Weinstein AM, Spencer KB, Duke BJ, Walp E, Kim Y-H, Sutliff RL, Bao H-F, et al. Pendrin modulates ENaC function by changing luminal HCO_3-. *JAmSocNephrol.* 2010;21(1928-41.

SUPPLEMENTAL DATA

Supplemental Table 1: Effect of IC *Nedd4-2* gene ablation on H^+-ATPase abundance and subcellular distribution in mouse CCD				
	Type A Intercalated Cells		Type B Intercalated Cells	
	Cre (-), floxed *Nedd4-2*, Wild type littermates	IC *Nedd4-2* null	Wild type	IC *Nedd4-2* null
Cell height, arbitrary units	1.63 ± 0.13	1.55 ± 0.05	1.55 ± 0.1	1.54 ± 0.05
Total cell expression (pixel intensity), arbitrary units, X 10^{-1}	1018 ± 125	944 ± 16	734 ± 101	748 ± 52
Apical expression ratio (expression in the apical 20% relative to total expression)	0.218 ± 0.016	0.209 ± 0.005	NA	NA
Basolateral expression ratio (expression in the basolateral 25% relative to total expression)	NA	NA	0.225 ± 0.011	0.214 ± 0.011
Values were determined using quantitative immunohistochemistry; N=5 mice in each group; NA, not applicable, P = NS. Mice consumed the NaCl-rich diet (1.4 meq/d NaCl) for 7 days before sacrifice.				

SUPPLEMENTAL FIGURES

Supplemental Figure 1: Intercalated cell *Nedd4-2* gene ablation produces little change in CCD H^+ secretion and no detectable change in apical H^+-ATPase immunolabel. Panel A: J_{tCO2} was measured in CCDs from IC *Nedd4-2* knockout (n=5) and wild type littermates (n=5) with either bafilomycin (5 nM) or vehicle in the perfusate. Solid lines indicate experiments in which vehicle was present in the first period and bafilomycin added in the second. The dashed lines show the reverse order, i.e. bafilomycin present in period one and then removed in period two. The right panel shows that the bafilomycin-sensitive component of $JtCO_2$ was low and not significantly different between groups.

Panel B shows a representative cortical collecting duct from an IC *Nedd4-2* null and a wild type littermate labeled for the α4 subunit of the H^+-ATPase. Arrowheads show H^+-ATPase immunolabel in the apical region of the cell, indicating type A intercalated cells. Arrows show H^+-ATPase immunolabel in the basolateral regions, indicating type B intercalated cells. Although H^+-ATPase expression varied among individual type A and type B intercalated cells, overall *Nedd4-2* gene ablation did not increase label intensity nor did it increase the relative label in the apical or the basolateral plasma membrane region of either intercalated cell subtype.

Supplemental Figure 2: IC *Nedd4-2* gene ablation increases pendrin immunogold label on the apical plasma membrane relative to the cytoplasm in type B intercalated cells of the CCD. The top panel shows gold (pendrin) label in representative type B intercalated cells taken from an IC *Nedd4-2* KO and a wild type littermate. The arrows indicate gold (pendrin) label on the apical plasma membrane,

whereas arrowheads indicate label in the subapical space. The insets mark regions of each micrograph shown at higher magnification in the lower panels.

Supplemental Figure 3: IC *Nedd4-2* gene ablation does not increase barttin label intensity per cell or increase label intensity in the basolateral membrane region. This figure shows barttin label (brown) in cortical sections from IC *Nedd4-2* null and wild type littermates. Sections were double labeled for pendrin (blue) to indicate type B and Non-A, non-B intercalated cells. The upper panels show pendrin and barttin label in cortical sections at low magnification. The regions circumscribed within a box indicate cortical collecting ducts shown at higher magnification in the lower panels. Arrows indicate pendrin-positive, type B intercalated cells, whereas arrowheads indicate pendrin-negative type A intercalated cells. As shown, there was no striking increase in intercalated cell bartin label intensity in the CCDs from IC *Nedd4-2* null relative to their wild type littermates.

Supplemental Figure 4: IC *Nedd4-2* gene ablation does not increase AE4 immunolabel. The upper panel shows sections from an IC *Nedd4-2* null and a wild type littermate that were labeled for AE4. The lower panel shows sections from each group at higher power that were labeled for both AE4 (brown) and for pendrin (blue). As shown, AE4 label intensity is more striking in pendrin positive (arrows) than in pendrin negative cells (arrowheads), which indicates greater expression in either type B or Non-A, non-B (arrows) than in type A intercalated cells (arrowheads). No AE4 label was detected in principal cells. IC *Nedd4-2* gene ablation did not increase AE4 label intensity nor did it increase the relative AE4 label in the region of the plasma membrane.

Supplemental Figure 5: Effect of NaCl intake on systolic blood pressure in IC *Nedd4-2* null and wild type mice. This figure shows systolic blood pressure measured by tailcuff in 6 IC *Nedd4-2* null and 6 wild type littermates following a standard 1% NaCl diet consumed at libitum. Blood pressure was then re-measured in these mice after 14 days of a 4% NaCl diet.

Supplemental Figure 1

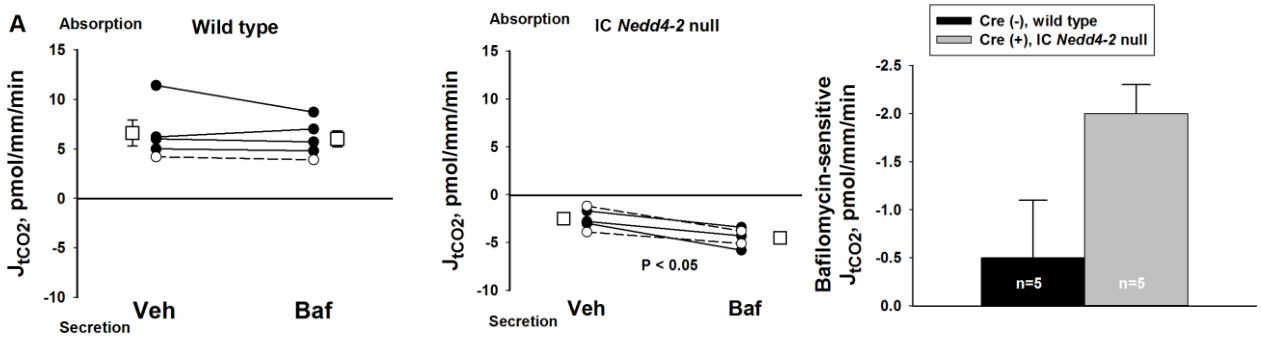

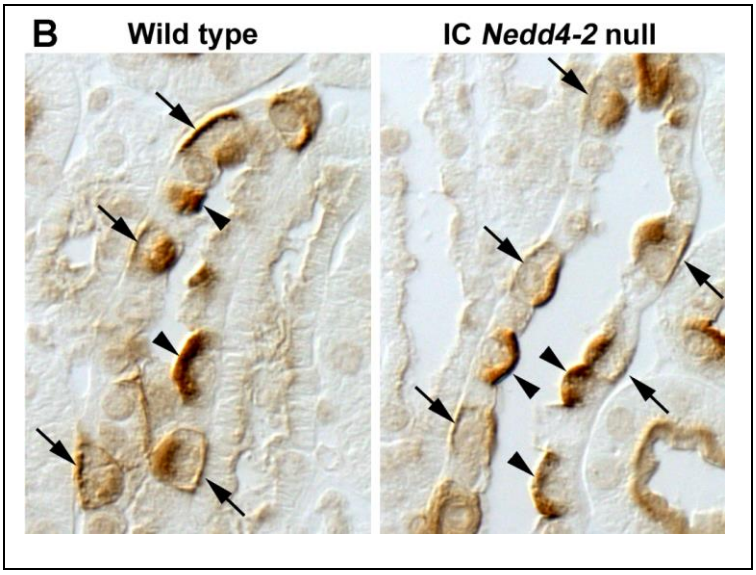

Supplemental Figure 2

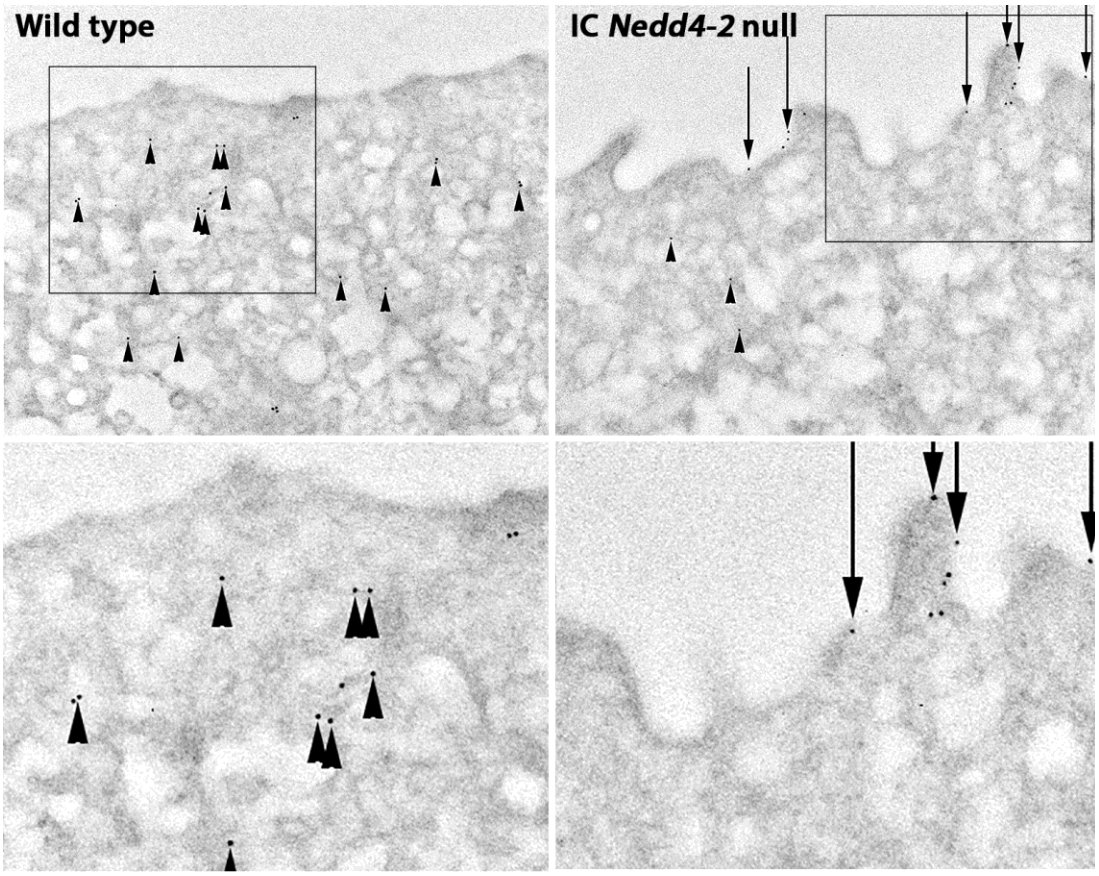

Supplemental Figure 3

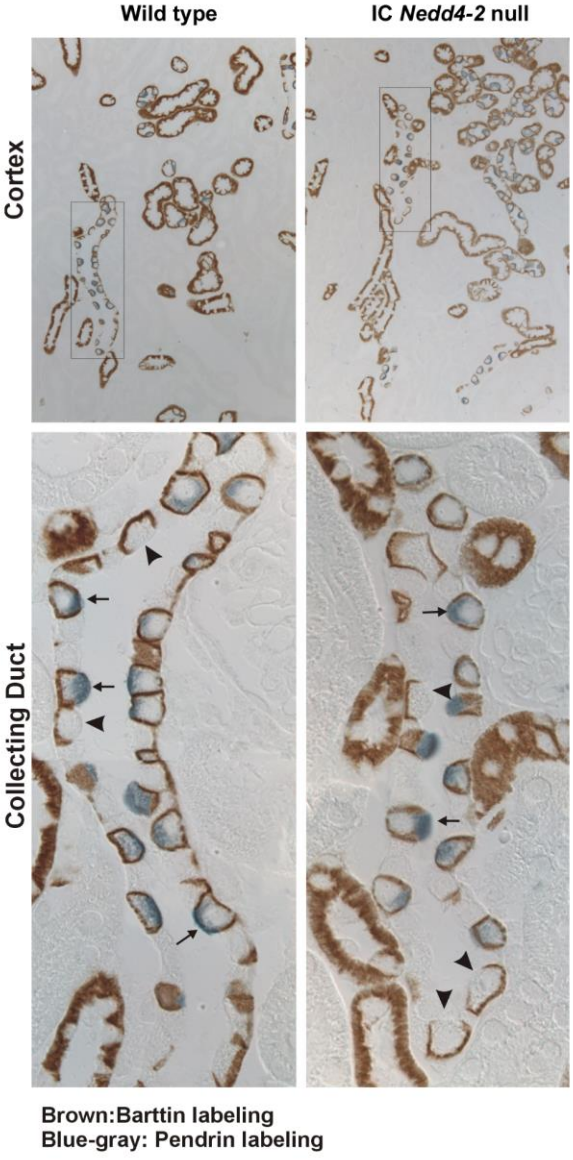

Supplemental Figure 4

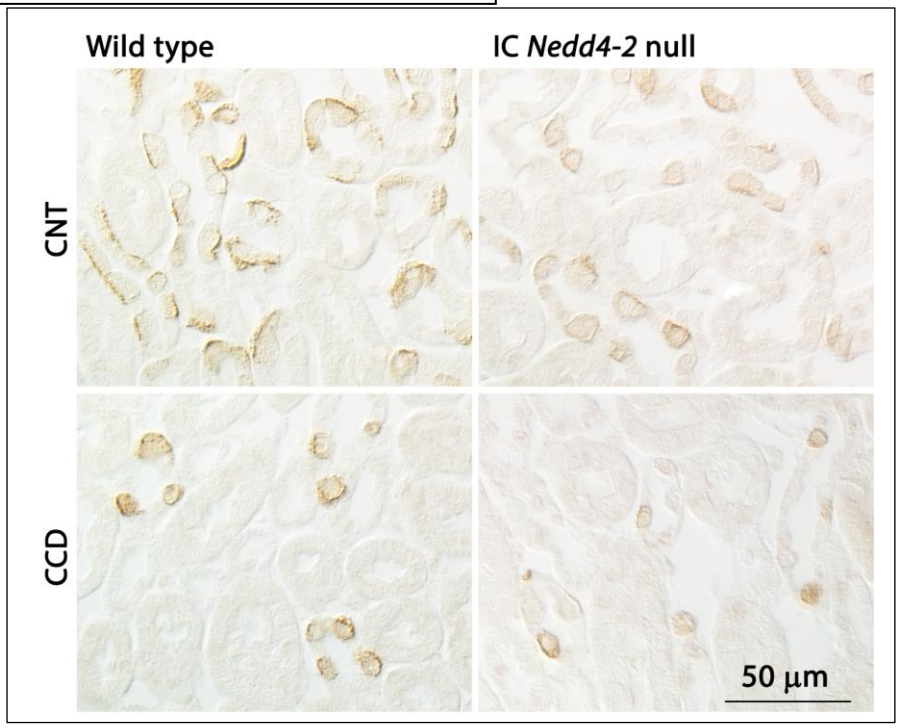

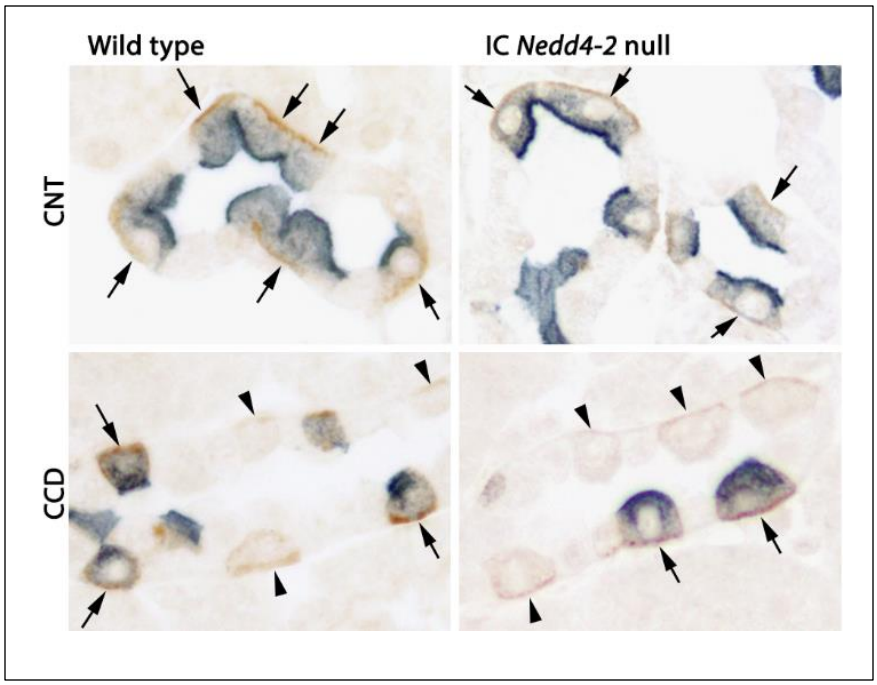

Supplemental Figure 5